Available online at www.sciencedirect.com

ScienceDirect

Procedia Engineering 10 (2011) 2621–2626

Engineering Procedia

ICM11

High Strength Engineered Alumina-Silicon Carbide Laminated Composites by Spark Plasma Sintering

F. De Genua* and V. M. Sglavo

DIMTI, University of Trento, Via Mesiano 77, 38123 Trento, Italy

Abstract

Spark Plasma Sintering was used to produce two engineered ceramic laminates in the SiC-Al_2O_3 system starting from tape casted composite layers. By changing the composition of the stacked laminae and the architecture of the laminate, tailored residual stress profile was produced after sintering and successive cooling. The laminates are sensible stronger than parent monolithic composite ceramic and show very limited strength variability which can be associated to the stable growth of surface defects before final failure as it is predicted by the apparent fracture toughness curve. Such shielding effect is also observed when macroscopic cracks are introduced by high load Vickers indentation.

Keywords: Laminates; Residual Stresses; Fracture; Spark Plasma Sintering; Alumina; Silicon carbide.

1. Introduction

The lack of reliability in mechanical strength of ceramics can be overcome by the design of laminated structures that are able to develop, upon processing, specific residual stress profile with maximum compression at specific depth from the surface. The arising fracture toughness curve can be responsible for surface defects stable growth and, consequently, for surface damage insensitivity that leads to outstanding mechanical performances for typical brittle materials such as ceramics. Using this approach, some oxide laminated structures have been recently investigated and very high reliability, in terms of Weibull modulus or minimum threshold strength, has been shown experimentally [1-5].

* Corresponding author. Tel.: +39-0461-282474 ; fax: +39-0461-281945 .
E-mail address: francesca.degenua@ing.unitn.it

 doi:10.1016/j.proeng.2011.04.437

Silicon carbide has been extensively used in the past as inert second phase to improve the mechanical properties of alumina ceramics [6,7]. The composites have been usually prepared by hot pressing to overcome limited densification and significant weight loss observed in pressureless sintering [8].
Spark Plasma Sintering (SPS) represents an innovative technology, which uses a pulsed direct electric current that passes through the graphite die to generate heat to sinter different material compositions. The electrical current propagation significantly improves heat-transfer resulting in a current activated sintering and, in particular, allowing high heating rates, lower processing temperatures and shorter holding times for the production of highly dense materials with good control of grain coarsening [9].
In the present work, following a previous research activity [10,11], silicon carbide was selected to graduate the thermal expansion coefficient of alumina due to its relatively low specific density that can allow the production of lighter components. Monolithic ceramic composite laminates and two engineered laminates were produced by Spark Plasma Sintering (SPS) and physical and mechanical properties were measured and correlated to structural features.

2. Experimental procedure

Commercially available high-purity α-Al_2O_3 (A-16SG, Alcoa Inc., Pittsburgh, PA, USA) and α-SiC (Sika ABR I F1500S, Saint-Gobain, Courbevoie, France) powders with an average particle size of 0.4 μm and 1.8 μm, respectively, were used in this work. Alumina/silicon carbide laminae with 0 ÷ 25 vol% SiC loads were produced and labelled as ASx where x is the volume content of the second phase (SiC). The green laminae were obtained by tape casting water–based slurries prepared using a two-stage milling/mixing procedure. The alumina dispersion was prepared ball milling the powder with deionised water and dispersant (Darvan C®, R. T. Vanderbilt Inc., Norwalk, CT, USA) - 0.4 mg/m^2 of active matter per unit area of alumina powder - for 24 h. Then, SiC powder was added and the suspension was milled for additional 24 h. The slurry was filtered through a 41 μm filter and de-aired for 30 min using a low-vacuum Venturi pump to remove air entrapped during the mixing stage. An acrylic emulsion (Duramax® B-1014, Rohm & Hass, Philadelphia, PA, USA) as binder and a low-T_g acrylic emulsion (Duramax® B-1000, Rohm & Hass, Philadelphia, PA, USA) as plasticizer were added to the dispersions and mixed for 30 min at 150 rpm. Three drops of 10 wt% wetting agent water solution (NH_4-lauryl sulphate, code 09887, Fluka Chemie AG, Buchs, Switzerland) were also added after 20 min of mixing to improve the tape spread onto the casting substrate. All suspensions were produced with powder content equal to 39 vol%. Binder content was always equal to 15.3 vol% and plasticizer was added in a volume ratio with respect to the binder equal to 1:2.
Tape casting was carried out using a double doctor-blade assembly (DDB-1-6, 6 in wide, Richard E. Mistler Inc., Yardley, PA, USA) with a speed of 1 m/min and two different blade heights, 250 μm and 100 μm. The tapes were casted on the polyethylene hydrophobic surface side of a composite film substrate (PET12/Al7/LDPE60, BP Europack, Vicenza, Italy) fixed on a rigid float glass plate. The relative humidity of the over-standing environment was set to 80% in order to control the drying of the tapes. Green tapes with smooth surfaces and uniform thickness of approximately 120 μm and 60 μm were therefore produced and disks of 30 mm nominal diameter were cut by a hollow punch. Monolithic green laminates were produced by thermo-compressing 34 identical 120 μm thick layers at 80°C under 30 MPa for 15 min.
A pre-sintering treatment useful for the burn-out of organic additives without oxidation of SiC was performed in Ar at 1000°C with a dwell time of 12 min. Each laminate was sintered by a SPS apparatus (Dr. Sinter 1050, Sumimoto Coal Mining Co., Tokyo, Japan) at 1700°C with a holding time of 2 min and a uniaxial pressure of 28.7 MPa. Heating rate of 100°C/min, vacuum level of 10^{-2} mbar and pulsed current (12 impulses of 3 ms on and 2 impulses of 3 ms off) were applied. Tapes with different thickness and composition were stacked together to obtain the engineered architectures labelled as AS-X and AS-Y shown in Fig. 1.

SPS compact disks were cut with a diamond blade in bars of 5 mm x 25 mm nominal dimensions, the provisional tensile load surface being perpendicular to the SPS axis. Four point bending tests were carried out using a universal mechanical testing machine (mod. 810, MTS Systems, Minneapolis, MN, USA) with an actuator speed of 0.2 mm/min and inner and outer span of 10 mm and 20 mm, respectively. For each laminate, 4-6 samples were considered. A certain number of engineered laminates were also pre-cracked by Vickers indentation before flexural test. Polished sections and fracture surfaces were then examined by optical microscopy (BH2-UMA, Olympus Optical Co. GmbH, Hamburg, Germany).

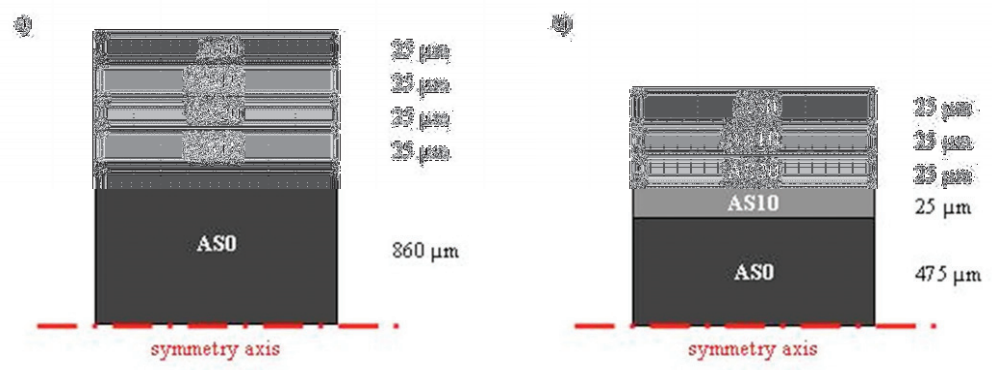

Fig. 1: Architecture (i.e. composition, stacking order and layers thickness) of the engineered alumina/silicon carbide multilayers (a) AS-X and (b) AS-Y. Dimensions are not in scale.

3. Residual stresses and apparent fracture toughness curve

The procedure used to design such laminates are described in details in previous works [1-3]. The properties of alumina and silicon carbide required for the design calculations can be obtained from NIST Structural Ceramics Database [12]. Fracture toughness was measured on monolithic composites by the conventional indentation fracture method [13]. Vickers indentations were produced using a load of 100 N.

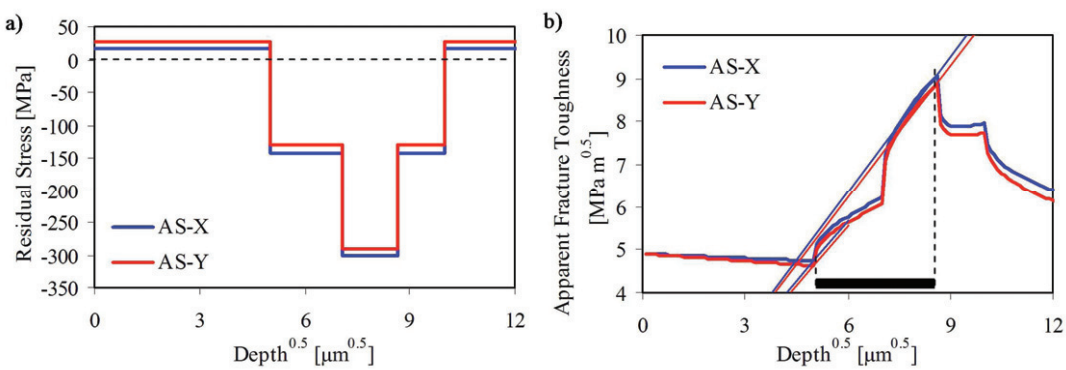

Fig. 2: Calculated residual stress profiles (a) and apparent fracture toughness curves (b) in the surface region of the engineered laminates AS-X and AS-Y. The straight lines corresponding to the design failure stresses and the minimum stresses required for crack propagation are also shown in (b) and used for the determination of the stable growth interval (horizontal bar).

On the basis of the elastic and thermal properties of the materials, the residual stress profiles frozen in the

engineered laminates after sintering and successive cooling can be evaluated [1-5] as shown in Fig 2(a). Similarly to previous situations where the material was tailored to manifest high mechanical reliability [1-5], the stress state is slightly tensile (17 MPa in AS-X and 28 MPa in AS-Y) on the surface while a considerable residual compression (302 MPa in AS-X and 291 MPa in AS-Y) occurs at a depth between 50 μm and 75 μm.
The apparent fracture toughness curves of the laminates associated with the residual stress profiles are shown in Fig. 2(b). A stable crack growth interval (from ≈ 25 μm to ≈ 75 μm) before final failure can be observed in both cases. One can also observe that the engineered laminates failure stress associated with the maximum apparent fracture toughness, graphically determined by the line through the origin intersecting the apparent fracture toughness curves at the maximum, are quite similar and equal to 530 MPa and 520 MPa for AS-X and AS-Y, respectively.

4. Results and discussion

The sintered composite materials always reached almost theoretical density. Observations of the laminates polished section under microscope confirmed the presence of limited porosity and showed homogeneous distribution of the two phases. Perfect adhesion between the initial layers was also observed both in monolithic and in the engineered laminates where layers of different composition were assembled (Fig. 3).

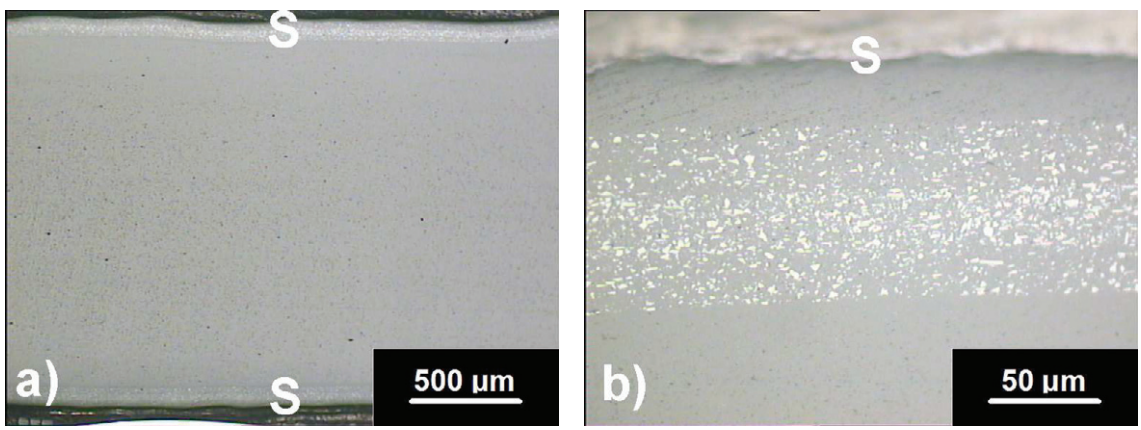

Fig. 3: Optical micrographs showing the polished section of the engineered laminate AS-X (a) and its architecture near the surface S (b).

Table 1. Strength measured on pure alumina (AS0) and on engineered laminates AS-X and AS-Y.

	Average strength (MPa)	Standard deviation (MPa)	Covariance (%)
AS0	417	116	27.8
AS-X	559	40	7.2
AS-Y	605	50	8.3

The engineered laminates AS-X and AS-Y showed similar average strength, as shown in Table 1, always sensibly larger than the resistance of pure alumina. One can observe that the design strength from Fig. 2(b) is slightly smaller than the measured failure stress, this pointing out an even more pronounced strengthening effect of the residual stress field which is probably not included in the calculation due to the

simple crack model considered here [1-5]. The strength variability (reported in Table 1 as covariance = average strength / standard deviation) is also sensibly suppressed in the engineered laminates, being always lower than 10%, in spite of the limited number of samples, five to six, used for the mechanical tests.

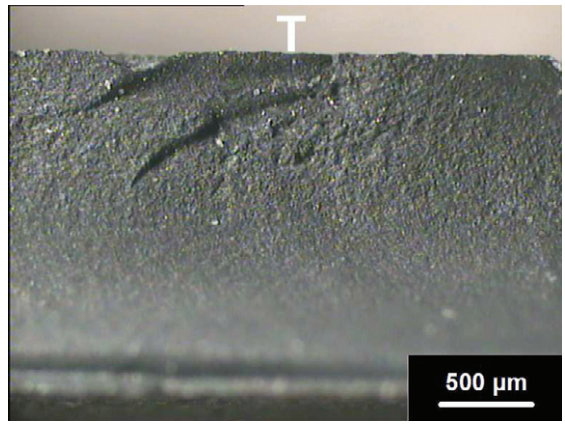

Fig. 4: Optical micrograph showing the fracture surface of the homogeneous alumina laminate. Initiation site is clearly visible on the right of the tensile surface (T).

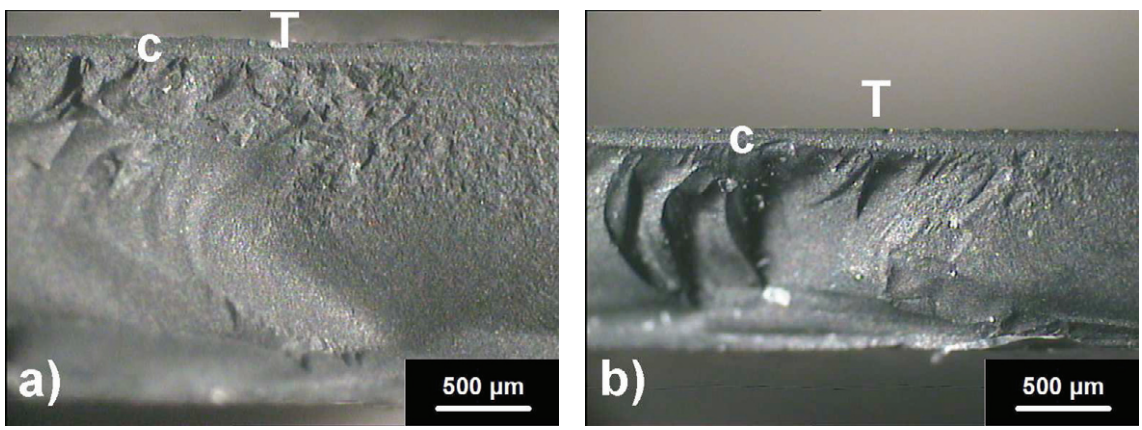

Fig. 5: Optical micrographs showing a particular of the fracture surface of the engineered laminates AS-X (a) and AS-Y (b). A smooth narrow region (c) with a through-thickness geometry is visible just beneath the tensile surface (T).

Examination of fractographic features in monolithic alumina samples showed typical fracture mirror around the critical flaws usually localized on the tensile surface (Fig. 4). Conversely, the engineered laminates showed a constant depth smooth area just beneath the tensile surface (Fig. 5) which can be attributed to the stable growth of a surface crack into a through-thickness flaw within the surface layer in residual compressive stress. Then, when critical condition for unstable propagation is reached, crack propagation restarts producing a fracture surface similar to what observed in the case of homogeneous samples broken at high loads. Such behaviour is therefore responsible for the limited variability of the strength which is not directly correlated to randomly distributed surface flaws.

The shielding effect pointed out for natural surface flaws is active also when macroscopic damages are produced on the surface of the engineered laminate. As a matter of fact, constant strength values around 550 MPa were obtained for both the engineered laminates also on samples damaged with Vickers

5. Conclusions

By modifying the composition and the architecture of SiC-Al_2O_3 composite laminae, two engineered laminates characterize by tailored residual stress profile were produced by Spark Plasma Sintering.
The laminates are sensible stronger than parent monolithic ceramic and show very limited strength variability which can be associated to the stable growth of surface defects before final failure as it is predicted by the apparent fracture toughness curve. Such shielding effect is also observed when macroscopic cracks are introduced by Vickers indentation.

Acknowledgements

The authors wish to acknowledge the support of Dr. F. Casari (K4Sint S.r.l – start-up of the University of Trento – , Pergine Valsugana, Italy) involved in laminates sintering.

References

[1] Sglavo V M, Paternoster M, Bertoldi M. Tailored residual stresses in high reliability alumina-mullite ceramic laminates. *J. Am. Ceram. Soc*. 2005;**88**:2826-2832.

[2] Sglavo VM, Bertoldi M. Design and production of ceramic laminates with high mechanical resistance and reliability. *Acta Mater.* 2006;**54**:4929-4937.

[3] Sglavo VM, Bertoldi M. Design and production of ceramic laminates with high mechanical reliability. *Composites: Part B* 2006;**37**:481-489.

[4] Costabile A and Sglavo VM. Influence of the architecture on the mechanical performances of alumina-zirconia-mullite ceramic laminates. *Adv. in Science and Technology* 2006;**5**:1103-1108.

[5] Leoni M, Ortolani M, Bertoldi M, Sglavo VM, Scardi P. Nondestructive Measurement of the Residual Stress Profile in Ceramic Laminates. *J. Am. Ceram. Soc.* 2008;**91**:1218-1225.

[6] Peters SY edt. *Handbook of composites*. London, U.K: Chapman & Hall; 1998, p. 307-332.

[7] Lee WE, Rainforth M. *Ceramic Microstructures – Property control by processing*. London, U.K.: Chapman & Hall; 1994, p. 509-570.

[8] Gadalla A, Elmasry M, Kongkachuichay P. High temperature reactions within SiC-Al2O3 composites. *J. Mater. Res.* 1992;**7**:2585-2592.

[9] Munir ZA, Anselmi-Tamburini U, Ohyanagi M. The effect of electric field and pressure on the synthesis and consolidation of materials: A review of the spark plasma sintering method. *J. Mater. Sci.* 2006;**4**:763-777.

[10] Sglavo VM, De Genua F, Molinari A, Casari F. Alumina – silicon carbide laminated composites by spark plasma sintering. *J. Am. Ceram. Soc.* 2009; **92**:2693-2697.

[11] Sglavo VM, De Genua F. High Reliability alumina – silicon carbide laminated composites by spark plasma sintering. In: R. Gerhardt, editor, *Properties and applications of silicon carbide,* Croatia: Intech Open Access Publisher; 2011, in press.

[12] NIST Structural Ceramics Database, www.nist.gov.

[13] Anstis GR, Chantikul P, Lawn BR, and Marshall DB. A Critical Evaluation of Indentation Techniques for Measuring Fracture Toughness: I, Direct Crack Measurements. *J. Am. Ceram. Soc.* 1972;**64**:533–8.